

## Sequence homology-based identification of paracetamol metabolizing enzymes in chicken liver homogenates for *in vitro* drug metabolism studies.

Niharikha Mukala<sup>1</sup>, Madhumita Aggunna<sup>2</sup> and Ravikiran S. Yedidi<sup>3,4,\*</sup>

<sup>1</sup>Multiomics-Infectious diseases branch, <sup>2</sup>Multiomics-Oncology & Immunotherapy branch, <sup>3</sup>Department of Intramural research core, The Center for Advanced-Applied Biological Sciences & Entrepreneurship (TCABS-E), Visakhapatnam 530016, A.P. India; <sup>4</sup>Department of Zoology, Andhra University, Visakhapatnam 530003, A.P. India. (\*Correspondence to R.S.Y.: tcabse.india@gmail.com)

**Keywords:** Paracetamol, acetaminophen, chicken liver, CYPs, SULTs, UGTs, sequence homology, drug metabolism, NMR.

*In vitro* drug metabolism studies are very critical in the preclinical drug discovery pipeline. During the recent coronavirus disease-2019 (COVID-19) pandemic, many research laboratories were severely affected by the shortage of reagents such as human liver microsomes, etc. In parallel, there was an urge to evaluate many new drugs for their potential as antiviral agents to treat COVID-19 patients warranting the need for alternate and reliable sources of drug metabolizing enzymes. In this study, we used the common broiler chicken (BCh) liver homogenates as the source of enzymes and evaluated the metabolism of paracetamol. Our proton NMR spectra demonstrate that the BCh liver homogenates were able to metabolize paracetamol. Additionally, we performed an extensive sequence homology-based bioinformatics survey and identified BCh homologs that might potentially be involved in the metabolism of paracetamol. Further, the binding profiles of paracetamol in the active sites of the homolog enzymes provided more insights into the drug metabolism by our docking studies. Taken together, our studies serve as a prototype for *in vitro* drug metabolism studies using BCh liver homogenates as a source of metabolizing enzymes in combination with bioinformatics. Our prototype from this study will be expanded to evaluate the metabolism of various classes of drugs in the future.

**Citation:** Mukala, N., Aggunna, M., and Yedidi, R.S. (2023). Sequence homology-based identification of paracetamol metabolizing enzymes in chicken liver homogenates for *in vitro* drug metabolism studies. *TCABSE-J*, Vol. 1, Issue 5:12-19. Mar 22<sup>nd</sup>, 2023. Epub: Oct 25<sup>th</sup>, 2022.



Coronavirus disease-2019 (COVID-19) has been an ongoing pandemic since the early 2020 with the omicron variant of the severe acute respiratory syndrome coronavirus-2 (SARS CoV-2) being the latest emerging mutant virus (<https://covid19.who.int/>). Many countries have witnessed lockdowns allowing only medical emergency vehicles on the streets. Other than hospitals/clinics and drug stores, most of the businesses were shut down denting the economies across the globe (1). Vaccinations are usually the most effective way to control viral pandemics (2). However, due to the emergence of variants in SARS-CoV-2, the efficacy of vaccines can be compromised. Recently we showed that mutations in the viral spike protein can lead to significant structural and topological changes thus altering the epitopes that are crucial for the efficacy of vaccines (3, 4). In light of the emergence of such variants, usage of antiviral drugs is also important to support the efficacy of vaccines especially in the case of the latest highly mutated variants such as the omicron family (5). Hence, preclinical drug discovery, including drug metabolism studies must go on even during the pandemic situation.

These studies become challenging during the pandemic where ordering and delivery logistics of research chemicals, reagents, etc. are severely affected. Additionally, lack of funding in low income countries and remote villages warrants designing an alternative and reliable approach for performing the drug metabolism studies in order to continue the monitoring of small molecule drug efficacies and toxicities. In this study, we used paracetamol (6, 7, 8) as a model drug to evaluate its metabolism *in vitro* using the broiler chicken (BCh) liver homogenate as a source of cytochrome P450 (CYP) enzymes (9, 10), sulfotransferases (SULT) and UDP-glucuronosyl transferases (UGT). As shown in Figure 1, paracetamol is typically metabolized in four major ways viz, glucuronidation, sulfation, oxidation and deacetylation resulting in paracetamol glucuronide, paracetamol sulfate, *N*-acetyl-*p*-benzoquinone imine (NAPQI) and *p*-aminophenol, respectively (9, 10). The <sup>1</sup>H-NMR spectra were obtained and analyzed to evaluate the metabolism of paracetamol incubated with the BCh liver homogenates at different concentrations.

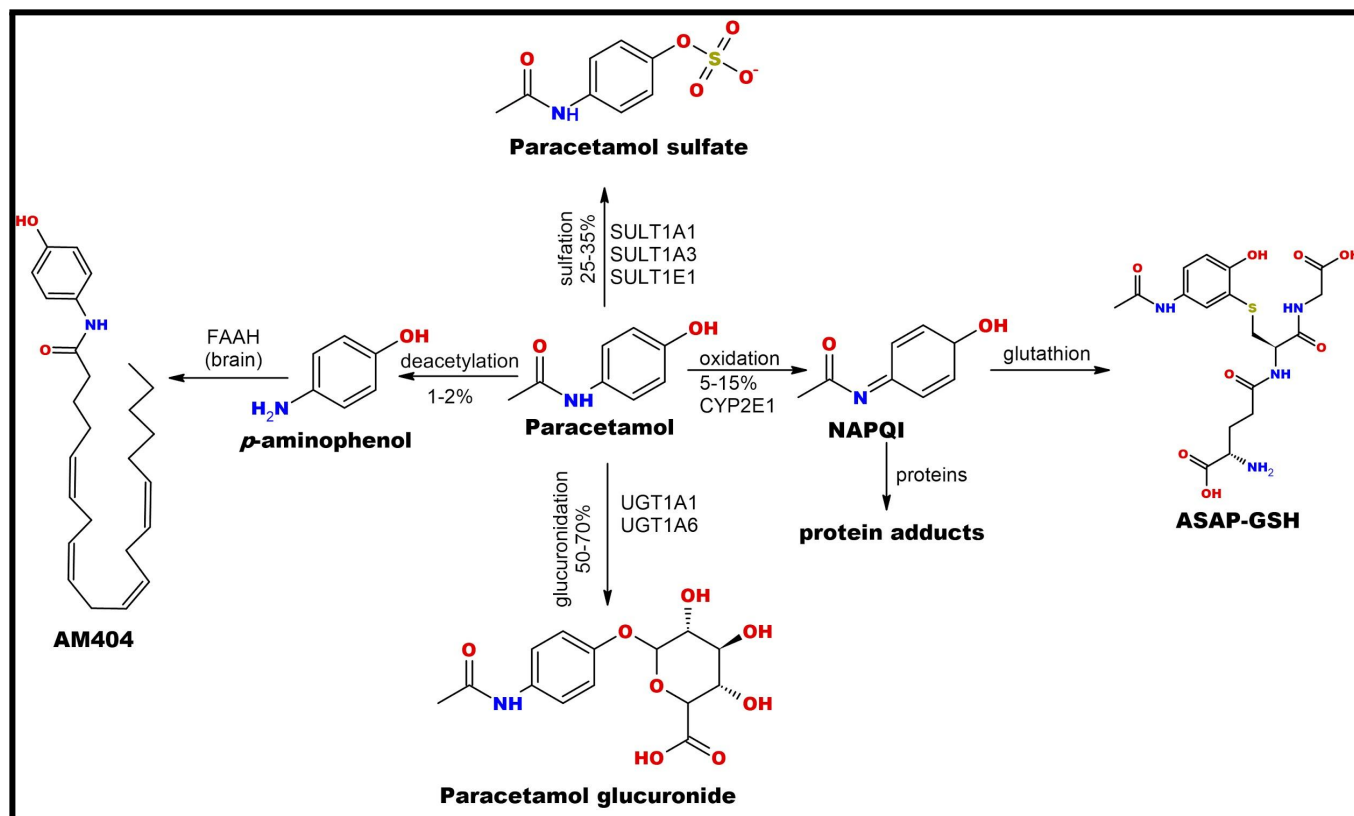


**Figure 1.** Overview of paracetamol metabolism in humans. This diagram mainly shows the three main types of metabolizing enzymes, CYPs, SULTs and UGTs. This diagram was generated using ChemSketch software from ACD Labs.

In this study we performed an extensive Bioinformatics analysis of the human and chicken CYPs, SULTs and UGTs with a goal to understand not only the sequence homology between the two but also the plausibility of using BCh liver homogenates as a reliable alternative source of drug metabolizing enzymes for preclinical drug metabolism studies.

### Materials & Methods:

**NCBI search for sequences:** The National Center for Biotechnology Information (NCBI) web server was used to search for the gene and protein sequences of both human and chicken enzymes that are the focus of this study. For each search, the RefSeq details were obtained to avoid any ambiguity in the sequences followed by the Genbank and Genpept reports for further technical details. The human CYP2E1 (Gene ID: 1571) and CYP3A4 (Gene ID: 1576) are involved in the metabolism of paracetamol (Figure 1). Similarly, there are 3 sulfotransferases and 2 UDP-glucuronosyltransferases involved in the metabolism of

paracetamol (Figure 1). The NCBI RefSeq protein accession IDs for human CYP2E1, CYP3A4, SULT1A1, SULT1A3, SULT1E1, UGT1A1 and UGT1A6 are given in Table 1.

**NCBI BLAST:** NCBI BLAST was performed by using the human protein sequences with RefSeq accession IDs given in Table 1. The BLAST (11, 12) search was streamlined for chicken sequences so that the results will display only for *Gallus gallus*. In order to choose the homolog from *G. gallus* for each of the human enzymes, the sequence identity was given first preference such that the best *G. gallus* sequence matching the corresponding human enzyme sequence with highest sequence homology can be identified. The second preference was given to the sequence coverage with respect to the total sequence length of the identified *G. gallus* sequence. Additionally, we preferred the target sequences with significantly low E values (<1.0). The final identified *G. gallus* protein sequence accession IDs along with the homology details are given in Table 2.

**Pairwise and multiple sequence alignments:** All pairwise alignments were performed using the global align algorithm in the NCBI-BLAST web server (11, 12, 13) and the multiple sequence alignments (MSA) were performed using the CLUSTAL OMEGA web server (14).

NW Score	Identities	Positives	Gaps	Score	Expect	Method	Identities	Positives	Gaps
1391	262/495(53%)	352/495(71%)	3/495(0%)	593 bits(1530)	0.0	Compositional matrix adjust.	301/503(60%)	386/503(76%)	7/503(1%)
Query 1	MSALGV-TVALLVAAFLLLVSHMRQVHSSWNLPPGPFPLTIGNLFQLELKNIPKSFTR	59	Query 1	MALIPDLAMETWlllavs1v1ly1yGTHSHGLFKKLGIPGPTLPFLGNILSYHGCFMF	60				
Sbjct 1	M LG +V LLV A LL + WR+ +P GP PLPTI+GN+ +++ KN+ K+ +	60	Sbjct 1	M L+PDL TWLLLA L LL LYG + FKKGIPGP PLPFLG L Y +G F	60				
Query 60	LAQRFQPVFTLYVGSQRMVVMHGKAVKKEALDYKDEFSGRGLP-AFHAHRDRGIIFNI	118	Query 61	DMECHKYKGVGFDYDQQVLAITDPMIKTVLKECVSYFNRRPFGPVGFKSAISI	120				
Sbjct 61	LA+++GPVF++ +G5 +VV+ GY+AVKKEALD DEF+ RG +P A++ GIIF+N	120	Sbjct 61	D C +KYKG+HG YDG+QPV+AI DP +IKT+LVKECVS FTNRR FG G ++SA+S+	120				
Query 119	GPTWKDIRRFSLLTLRNYMGKQGNESRIQREAHFLLEALRKTQGGPDPFTLIGCAPCN	178	Query 121	ADEEWRKRLSLLSPTFTSGKLEHMPVIAAQVGDVLRNLRRAETGKPVTLKDFGAYS	180				
Sbjct 121	W +RRF+L+TLRN+GMGK+ E RIQ EA LLE + KT+ PFDPTF + CA N	180	Sbjct 121	A D++WKR+R++LSPTFTSGKLEH PII YGD LV+N+ ++ + +K +FGAYS	180				
Query 179	VIADILFRKHFYNDKFLRLMYLFNFHLLSTPHLQYNIFFSLHYLPGSHRVIKIN	238	Query 181	MDVITSTSFVGNIDSLNIPQDPFVNTKLL1+fd1dppf1SITVFPFLIPIELVNLICV	240				
Sbjct 181	VI I+F K +DY D+KFL LM N F++++ W QLY F L YLPG H + K	240	Sbjct 181	MDV+ STSF V+IDS++ P DPFV N +K L+F FL+P + I +FPF+IP+LE +H+ +	240				
Query 239	VAEKEVSVSRVKEHHQSLDPNCPDLTCLLVEHEKESAEALRYTHDITVTVADLFF	298	Query 241	FPREVTNFRKSVKRMKESRLEDTQKRVDFLQIMIDSQN-----SKETESHKALSOL	293				
Sbjct 241	+ VK +V+E VK H SLDP+ P+D DC L +M++EK ++ + M + + DLF	300	Sbjct 241	P +V +F +M+K+ R E RVDFLQIMIDSQ+ ++E +S+K+LSD	300				
Query 299	AGTETTSTTLRYGLLILMKPYEIEEKLHEEIDRVIGSRIPAIKDRQEMPYDAVVHEIQ	358	Query 294	ELVAQSIIIFAGYETTSSVLSFIMYELATHPDVQQLQEEIDAVLPHKAPPTVDTLQI	353				
Sbjct 301	AGTETTSTT RYGLL+L+KYP+I+EK+ EEIDRV+G SR P + DR +MPY DAVVHEIQ	360	Sbjct 301	E++AQ++ F+FAGYETTSS LS+I Y LA HPDQV++LQ+EIDA LPHKA PTY+ V+QI	360				
Query 359	RFITLVPSPHPEATRODTRFRGVLIPKQVTVVPTLDSVLQYNDQEPDFPEKFKPEHFNEN	418	Query 354	EYLDRIWVNIETLRLFIAMRLERVCKKDVIEINGFIPKGVMMIPSYALHRDQVYTEPEK	413				
Sbjct 361	RFITL+P+LPH T+D FR Y+IPKGT V+P L + LYD+EFF+P +F P HFLN+N	420	Sbjct 361	EYLDRIWVNESLRLHPPGGRIERICCKTVEFNGVTIPKDMVNIYALHRDPAYWPKPEE	420				
Query 419	GFKFYSDYFPKPFSTGKRVCAGEGLARMEFLLLCAILQHFNLPVDPKIDILSPHIGF	478	Query 414	FLPERFSKKNKIDIPYIYTPFGSGPRNICGMRFALMNLKALIRVLQNFSPKCKETQI	473				
Sbjct 421	G F + SD+F PFS GKR+C GEGLARME+FULL ATIQ+F LKP++ P++ ++P G	480	Sbjct 421	F RPERFSKNGENIDPYTF LFGAGPRNICGMRFALLIVKVMVLLQNFSPKCKDPTI	480				
Query 479	GCIPPRYKLCVPIRS 493		Query 474	PLKLSLGLLQPEKPVVVKVESR 496					
Sbjct 481	G +PP Y+LC IPR 494		Sbjct 481	PL L G +QP+KP++LK+ R 503					

Figure 2. Pairwise alignment of human CYP2E1 vs. chicken CYP2C18 (left) and human CYP3A4 vs. chicken CYP3A80 (right).

Pairwise alignments for the human vs. chicken protein sequences given in Table 1 are detailed in Figures S1 to S7. The pairwise alignment of human and chicken CYPs are shown in Figure 2. MSA for SULT1A1 isoforms is given in Figure S8. MSA for human SULTs is given in Figure S9. MSA for human UGTs is given in Figure S10.

**CYP homology modeling:** Due to the unavailability of experimentally determined structure for the CYP-paracetamol complex, SWISS MODEL web server (15, 16) was used to build the 3-dimensional CYP models. The FASTA sequences for human CYPs 2E1 and 3A4 as well as for chicken CYPs, 2C18 and 3A80 were used as input for the SWISS MODEL web server to calculate the homology models. Experimentally determined structures downloaded from the protein data bank (<https://www.rcsb.org>) were used wherever possible.

**Paracetamol docking:** AutoDock-Vina (17) was used for paracetamol (ligand) docking against the human (CYP2E1 and CYP3A4) and chicken (CYP2C18 and CYP3A80) receptors. Docking was performed as described previously (17, 18). The AutoDock tools (version 1.5.7) was used to set the docking grid box, a virtual box of dimensions that is set to cover the active site of the macromolecule/receptor, including the Heme ring. Docking grid parameters are given in Table S1. Vina was used for exhaustive conformational sampling. The output docking poses were manually analyzed for proper orientations in the active site and were chosen for further analysis. The corresponding binding affinities of the

docking poses were also considered (Table 3) to compare the binding of paracetamol in humans vs. chicken CYPs. The best binding poses for all 4 CYPs for paracetamol are shown in Figure 3.

**Preparation of BCh liver homogenate:** The BCh raw liver that was used in this study was purchased from a local butcher/meat shop that sells chicken liver as a delicacy. The BCh liver was homogenized into a paste using a mortar and pestle in the presence of prechilled 1X TAE buffer that was added in aliquots making up to the final volume of 30 ml. This volume was chosen so that the final slurry was easily transferable using laboratory pipettes for the ease of further experiments. The slurry was then carefully aliquoted into 5 tubes @ 6 ml per tube.

**Paracetamol incubation with BCh liver homogenate:** Paracetamol was used as the model drug for the current metabolism studies using the BCh liver homogenates. Over the counter paracetamol tablets were crushed into fine powder using a clean dry mortar and pestle. The powdered tablet was then weighed and added to the five tubes containing BCh liver homogenate prepared above. Tubes 1 to 5 received 0.01 g, 0.1 g, 0.25 g, 0.5 g and 1.0 g of powdered tablets, respectively. Each tube was thoroughly mixed by brief vortexing at lower speed to obtain a homogeneous slurry containing the BCh liver homogenate and the powdered tablet. An additional tube containing 1.0 g of powdered tablets homogenized with 6 ml. of 1X TAE buffer without the BCh liver homogenate was prepared as a control. All 6 tubes were incubated at 37°C overnight. The tubes were then taken out of the incubator and processed further to extract paracetamol and its metabolites during the incubations.

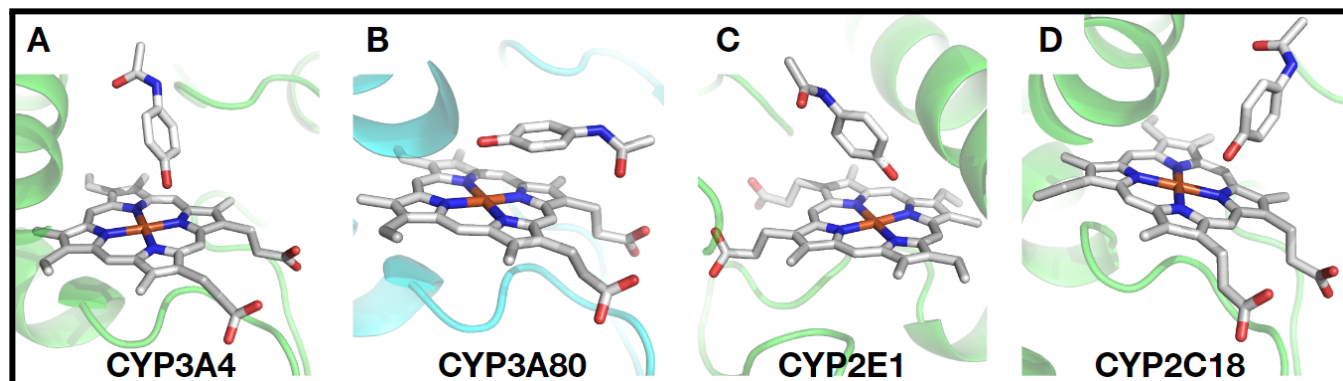


**Figure 3.** Docking poses of paracetamol in the active sites of CYP enzymes. Panels A and B show the paracetamol binding in the active site of human CYP3A4 and its chicken homolog, CYP3A80, respectively. Panels C and D show the paracetamol binding in the active site of human CYP2E1 and its chicken homolog, CYP2C18, respectively. In all panels the protein is shown as a cartoon in the background while the heme ring along with the paracetamol is shown as stick models with white carbon atoms, red oxygen atoms, blue nitrogen atoms and the iron atom in the middle of the heme ring is shown in blood red color.

Sl. No.	Human enzyme	NCBI Accession ID	Chicken Homolog	NCBI Accession ID
1	CYP2E1	NP_000764.1	CYP2C18	NP_001001752.2
2	CYP3A4	NP_059488.2	CYP3A80	NP_001316437.2
3	SULT1A1	NP_001046.2	SULT1D1	XP_040526865.2
4	SULT1A3	NP_808220.1	SULT1D1	XP_040526865.2
5	SULT1E1	NP_005411.1	SULT1D1	XP_040526865.2
6	UGT1A1	NP_000454.1	UGT1A1_X5	XP_040532293.1
7	UGT1A6	NP_001063.2	UGT1A9_X4	XP_040532291.1

**Table 1.** NCBI accession ID numbers for the human and the corresponding homologs from chicken paracetamol metabolizing enzymes focused on in this study.

Sl. No.	Human/chicken enzymes	Sequence Homology	Positives	Gaps
1	CYP2E1 / CYP2C18	51%	68%	4.0%
2	CYP3A4 / CYP3A80	56%	72%	6.0%
3	SULT1A1 / SULT1D1	61%	77%	0.0%
4	SULT1A3 / SULT1D1	59%	75%	0.0%
5	SULT1E1 / SULT1D1	62%	80%	0.0%
6	UGT1A1 / UGT1A1_X5	67%	79%	0.2%
7	UGT1A6 / UGT1A9_X4	61%	73%	1.0%

**Table 2.** Sequence homology of human vs chicken enzymes. (Details: Figures S1 to S7).

**Preparation of extracts:** Preparation of extracts was performed using a modified protocol published before (19). The contents of all 6 tubes (including the control) were briefly centrifuged at 13,000 rpm to pellet the particulate matter and the clear supernatant (labeled as supernant-1) was carefully transferred into new tubes. The pellets were then resuspended in 60% methanol solution and were boiled at 95°C briefly for 5 min. in the chemical fume hood to avoid the methanol vapors with intermittent mild shaking. The samples were then centrifuged at 13,000 rpm for 10 min. to pellet all the cellular debris. The methanol containing supernatants were carefully collected and transferred into new tubes labeled as supernant-2. The supernatant-1 for all 6 tubes were air dried and methanol extraction was performed as described above using 60% methanol solution. These extracts were then mixed with the supernatant-2 individually for all 6 tubes and the solvents were evaporated using a rota-evaporator. The final samples were prepared further for NMR studies.

**NMR sample preparation:** The dried product after the solvent evaporation was then dissolved in 1 ml. of deuterated-DMSO (DMSO-d6). The volume of DMSO-d6 was kept constant in all 6 tubes to maintain consistency in the extraction and NMR sample preparation protocols although the current study is purely qualitative based on the proton NMR spectra of the 6 samples. The DMSO-d6 containing the extracts was then carefully transferred into NMR tubes for data acquisition.

**NMR Spectroscopy:** BRUKER Ascend 400 MHz magnet was used for the acquisition of <sup>1</sup>H-NMR spectra for all the 6 samples (including the control without BCh liver homogenate). The FIDs were deconvoluted and fourier transformed into the individual spectra using TopSpin software. All proton spectra are given in Figures S11 to S16. A comprehensive diagram of all peaks from 6 samples are shown in the hand-drawn circular plot (20) along with their correlations in Figure 4.

Sl. No.	Human/chicken docking receptors	Binding affinity (kcal/mol.)
1	CYP2E1	-6.3
2	CYP3A4	-5.0
3	CYP2C18	-5.2
4	CYP3A80	-4.9

**Table 3.** Paracetamol-CYP docking results. (Details of docking parameters: Table S1).

## Results and Discussion:

*Sequence homology between human and chicken CYPs:* The human enzymes that are involved in paracetamol metabolism (Table 1) were used as the query sequences in NCBI BLASTp with a focus on identifying the chicken homologous enzymes. Multiple protein sequences from chicken were obtained as search results for each of the 7 human enzymes listed in Table 1. The best homologous sequences from chicken (Table 1) were chosen based on several factors such as the sequence identity, coverage, length of the query, E value, etc. as described in the material and methods section of this study. As shown in Figure 2, the human CYP2E1 has a sequence homology of 51% with an overall 68% positives and 23 gaps aligned with the chicken CYP2C18. The human CYP3A4 showed a sequence homology of 56% with an overall 72% positives and 31 gaps aligned with the chicken CYP3A80 (Figure 2). The sequence homology details of all human paracetamol metabolizing enzymes aligned with the chicken enzymes are given in Table 2 (for details please see Figures S1 to S7). All the chicken homologs have >50% sequence homology with <10% gaps in the sequences compared to the query human sequences suggesting that these chicken sequences can be considered further with confidence.

Some of the human paracetamol metabolizing enzymes such as SULT1A1 have multiple isoforms. In such cases, all the isoforms were aligned using CLUSTAL OMEGA first to identify any sequence discrepancies. Nine out of 10 human SULT1A1 isoforms were completely aligned with 100% sequence homology and no gaps (Figure S8). The tenth isoform was not included because it is a truncated form. The isoform 1 was considered for further BLAST search in order to identify the chicken homolog. As shown in Table 1, the chicken SULT1D1 was chosen as a homolog for all three human SULTs (1A1, 1A3 and 1E1) because the human SULT1A1 and SULT1A3 show a sequence homology of >92% without any gaps (Figure S9) although the overall sequence homology among all three human SULTS is almost 49% (Figure S9). Moreover, the

chicken SULT1D1 showed an average sequence homology of >60% against the human SULTs without any gaps (Table 2). The human UGTs showed a sequence homology of >68% with <0.5% gaps (Figure S10). Both UGT1A1 and UGT1A6 from humans showed sequence homologies of >60% with the chicken UGT1A1 and UGT1A9, respectively suggesting that these homologs can be confidently used for further evaluations.

*Binding profiles of paracetamol in human and chicken CYPs:* In order to analyze the binding profiles of paracetamol in the active sites of the human and chicken CYPs, the 3-dimensional molecular models were generated for all 4 CYPs listed in Table 1. Due to non availability of any structural data for CYP-paracetamol complex in the protein data bank, we generated the molecular models for CYPs in this study. Moreover, using the molecular models for all 4 CYPs gives consistency in docking avoiding any model vs. structure bias. Followed by the docking, each binding pose of paracetamol was manually observed and the final binding pose for further analysis was chosen accordingly (Table 3). As shown in Table 3, the binding affinity of paracetamol was found to be similar towards all four CYPs analyzed in this study. Highest binding affinity for paracetamol was found to be in the active site of the human CYP2E1 (-6.3 kcal/mol.) and the lowest binding affinity was found to be against the chicken CYP3A80 (-4.9 kcal/mol.). The difference in binding affinity values of paracetamol against the human CYP2E1 and its chicken homolog, CYP2C18 is 1.1 kcal/mol. while the difference in paracetamol binding affinity against the human CYP3A4 vs its chicken homolog, CYP3A80 is 0.1 kcal/mol. These results suggest that paracetamol can not only bind in the active sites of the chicken homologs of human CYPs but also exhibit similar binding affinities that are comparable with that of the human CYPs.

*In vitro proton-NMR-based evaluation of paracetamol metabolism:* Paracetamol was used as a model drug to test the *in vitro* drug metabolism using the BCh liver homogenate as a source of metabolizing enzymes. In order to evaluate the metabolism, the proton-NMR spectra (Figures S11 to S16) were obtained and compared. We performed a qualitative analysis without quantifying the proton peaks in these spectra and summarized our finding in Figure 4. As shown in Figure 4, a total of 6 concentric circles were drawn to represent the 6 spectra that were obtained for paracetamol concentrations, 0.01 g, 0.1 g, 0.25 g, 0.5 g, 1.0 g and control. The total number of peaks for each of the 6 samples were plotted as a histogram containing color coded bars. Correlation lines are drawn from the bottom of each bar connecting to the peak positions for each of the 6 samples. Additionally, the number of peaks in each sample that are divided into

various chemical groups such as aliphatic, aromatic, etc. are also given in the circular plot.

center of the circle to the outer circumference. These axes show ppm 1-3.5 ppm on the top left side of the plot and

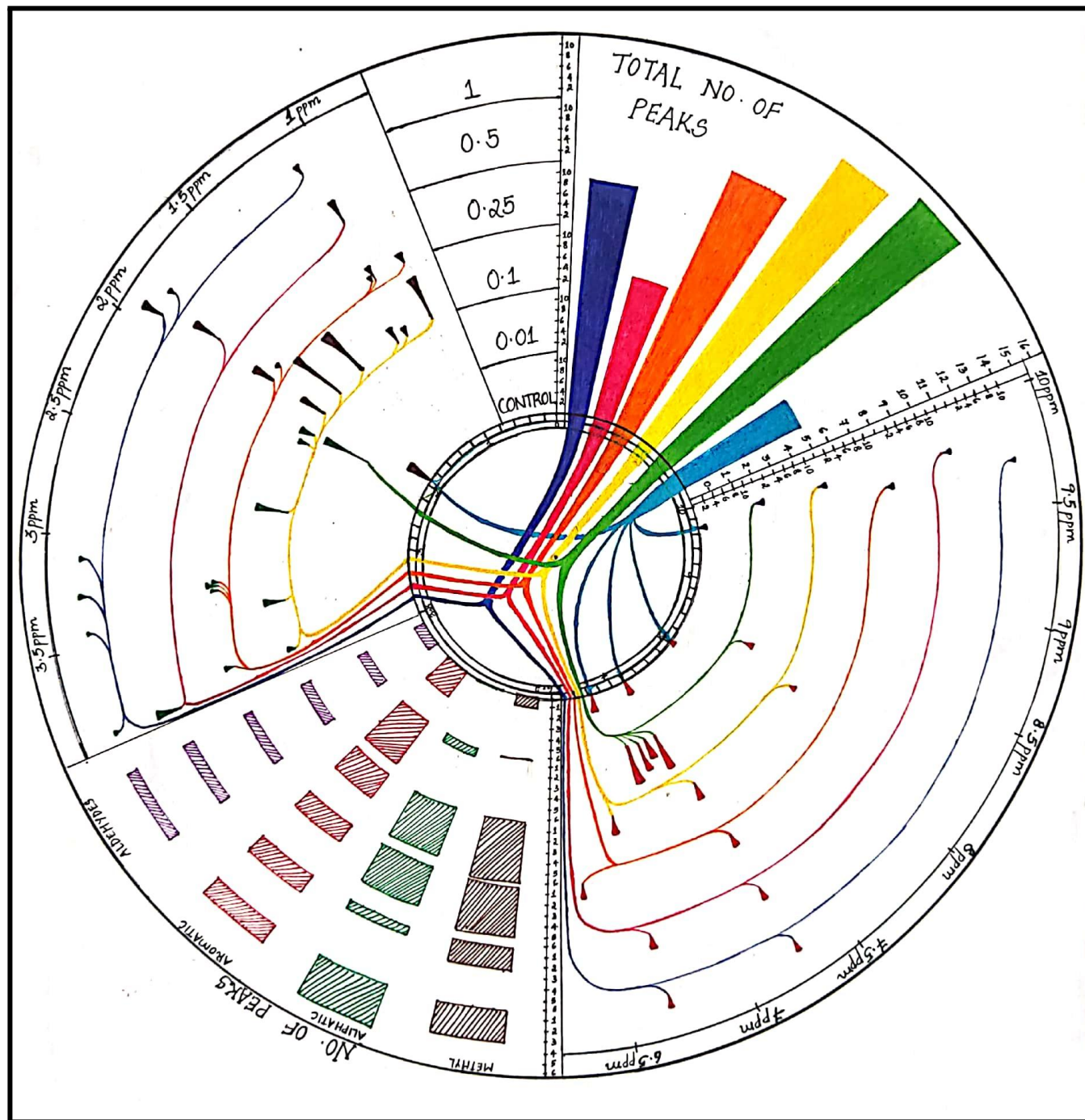


**Figure 4.** Hand-drawn circular plot showing the qualitative analysis of the proton NMR spectra. The 6 concentric circles indicate the x-axes for the proton NMR spectra of the 6 samples: control, 0.01 g, 0.1 g, 0.25 g, 0.5 g, 1.0 g from the

6.5-10 ppm on the bottom right side of the plot. The histogram contains color coded bars (cyan-control, green-0.01 g, yellow-0.1 g, orange-0.25 g, red-0.5 g and blue-1.0 g) representing the number of peaks in each sample

along with correlation lines connecting to the peaks represented by small wedges. The number of aromatic, aliphatic, etc. peaks are shown for each axis/sample using broken shaded bars. Individual y-axes are given for the data.

Evidently, the paracetamol concentrations 0.01 g, 0.1 g and 0.25 g displayed more proton peaks in their spectra compared to the control, while the paracetamol concentrations 0.5 g and 1.0 g yielded relatively lower number of proton peaks yet more peaks compared to the control. While the aldehyde and aromatic peaks were seen in all 6 samples, the aliphatic/methyl peaks were seen in variable proportions. Thus, our qualitative analysis of the number of peaks suggest that the paracetamol is indeed metabolized by the BCh liver homogenate containing the drug metabolizing enzymes.

**Discussion:** In this study, we performed an extensive Bioinformatics evaluation of the sequence homology between the human paracetamol metabolizing enzymes listed in Table 1 and the chicken enzymes in order to support our *in vitro* proton NMR-based paracetamol metabolism studies performed using the BCh liver homogenate as the source of enzymes. In the initial round of unbiased NCBI BLASTp search using human sequences as queries, we were unable to obtain any corresponding chicken sequences with reasonable homology (details not mentioned here). Hence, in the second round of the NCBI BLASTp search, we included chicken as the target organism as the subject where we obtained results with high sequence homology which were discussed in this article. Although all the E values for our NCBI BLASTp searches were well below 1.0, we did not give preference to the E values but we focused on the sequence identities and query coverage rather, in the context of the total length of the sequence under analysis. In this way, we were able to obtain the chicken homologs within a reasonable sequence homology range of 51% to 67% (Table 2) that showed <10% gaps and >68% positives. Typically higher sequence homology can be expected in mammals such as sheep, goat, etc. rather than chicken (avian) due to longer evolutionary distance from the humans. However, the BCh liver availability is more plausible at the local meat shops rather than that of a sheep or goat. In order to support the reasonable sequence homology between the human and chicken enzymes, we further evaluated the binding orientations and related binding affinities of paracetamol docked into the active sites of both human and chicken CYPs. As shown in Figure 3, we successfully obtained the docked poses of paracetamol in the active sites of all four CYPs that are listed in Table 1. These docking models are specifically important in this study due to the lack of any structural data in the protein data bank related to paracetamol binding to the CYPs. As of September 2022, we were able to obtain 10 structures in the

protein data bank that contain paracetamol but none of them contained CYPs. The binding affinities for paracetamol bound in the active sites of human CYP2E1, human CYP3A4, chicken CYP2C18 and chicken CYP3A80 were -6.3 kcal/mol., -5.0 kcal/mol., -5.2 kcal/mol. and -4.9 kcal/mol., respectively. The docking results suggest that paracetamol can bind both human and chicken CYPs with similar binding affinities thus supporting our *in vitro* proton NMR-based paracetamol metabolism studies performed using the BCh liver homogenate.

Our study demonstrates the qualitative analysis of paracetamol metabolism using BCh liver homogenate containing the drug metabolizing enzymes. Considering the similarity in paracetamol binding affinities docked against the human vs. chicken CYPs, we safely conclude that the paracetamol is indeed metabolized by the homologs identified in this study (Table 1). However, we did not focus on the quantitative analysis of paracetamol metabolism by the BCh liver homogenate in this study because we are currently in the process of evaluating the genetic polymorphisms in human vs. BCh CYPs including the paracetamol-protein adducts (PPA) (21, 22) studies to build a comprehensive open source database that one can refer to during the *in vitro* drug metabolism studies. Our current study establishes direct support from the Bioinformatics related sequence homology analysis followed by the 3-dimensional docking analysis for our *in vitro* paracetamol metabolism evaluation using BCh liver homogenate. Our future investigation will include similar studies with other small molecules related to cancer chemotherapy and antiviral agents in order to establish a strong platform for utilization of BCh liver homogenate in the place of human liver microsomes. Paracetamol has been shown to form protein adducts especially with the cysteines. These PPA may interfere with the normal protein function and may even be fatal some times. Whether a similar PPA formation mechanism exists in the BCh is yet to be evaluated in the future.

**Acknowledgements:** We thank Dr. Muralikrishna Muthyala and Mr. Ayyappa Kumpatla from the College of Pharmaceutical Sciences, Andhra University, Visakhapatnam for helping us with the NMR facility located in the Physics department of Andhra university, Visakhapatnam. We thank Mr. Ayyappa Kumpatla for helping us with NMR data acquisition and processing the FIDs to obtain the final proton spectra. We thank The Yedidi Institute of Discovery and Education, Toronto for scientific collaborations.

**Conflict of interest:** The authors declare no conflict of interest in this study. However, this research article is an ongoing project currently at TCABS-E, Visakhapatnam, India.

**Author contributions:** N.M. performed Bioinformatics analysis, prepared BCh liver homogenates, extracts and obtained the <sup>1</sup>H-NMR spectra for all samples. M.A. performed Bioinformatics analysis and docking studies including the identification of binding poses for paracetamol. R.S.Y. is the principal investigator who designed the project, trained both N.M. and M.A. in Bioinformatics, docking and *in vitro* experiments, secured required material for the project, provided the laboratory space and equipment needed for the experiments, wrote and edited the manuscript.

## References

- Shang Y, Li H and Zhang R (2021) Effects of Pandemic Outbreak on Economies: Evidence From Business History Context. *Front. Public Health* 9:632043.
- Watson, O. J., Barnsley, G., Toor, J., Hogan, A. B., Winkill, P., & Ghani, A. C. (2022). Global impact of the first year of COVID-19 vaccination: a mathematical modelling study. *The Lancet. Infectious diseases*, 22(9), 1293–1302. doi: 10.1016/S1473-3099 (22)00320-6.
- Addala S, Vissapragada M, Aggunna M, Mukala N, Lanka M, Gampa S, Sodasani M, Chintalapati J, Kamidi A, Veeranna RP, Yedidi RS. Success of Current COVID-19 Vaccine Strategies vs. the Epitope Topology of SARS-CoV-2 Spike Protein-Receptor Binding Domain (RBD): A Computational Study of RBD Topology to Guide Future Vaccine Design. *Vaccines* (Basel). 2022 May 25;10(6):841.
- Vissapragada M, Addala S, Sodasani M, Yedidi RS. Major structural deviations in the receptor binding domain of SARS-CoV-2 spike protein may pose threat to the existing vaccines. *TCABSE-J* 2021. Apr 13th; 1(1):12-14.
- Li P, Wang Y, Lavrijsen M, Lamers MM, de Vries AC, Rottier RJ, Bruno MJ, Peppelenbosch MP, Haagmans BL, Pan Q. SARS-CoV-2 Omicron variant is highly sensitive to molnupiravir, nirmatrelvir, and the combination. *Cell Res*. 2022 Mar;32(3):322-324. doi: 10.1038/s41422-022-00618-w.
- Fukuhara, K., Ohno, A., Ando, Y., Yamoto, T., & Okuda, H. (2011). A <sup>1</sup>H NMR-based metabolomics approach for mechanistic insight into acetaminophen-induced hepatotoxicity. *Drug metabolism and pharmacokinetics*, 26(4), 399–406.
- Zhao, L., & Pickering, G. (2011). Paracetamol metabolism and related genetic differences. *Drug metabolism reviews*, 43(1), 41–52.
- Mazaleuskaya, L. L., Sangkuhl, K., Thorn, C. F., FitzGerald, G. A., Altman, R. B., & Klein, T. E. (2015). PharmGKB summary: pathways of acetaminophen metabolism at the therapeutic versus toxic doses. *Pharmacogenetics and genomics*, 25(8), 416–426.
- Yang Y, Wong SE, Lightstone FC (2014) Understanding a Substrate's Product Regioselectivity in a Family of Enzymes: A Case Study of Acetaminophen Binding in Cytochrome P450s. *PLoS ONE* 9(2): e87058.
- Kalsi, S. S., Wood, D. M., Waring, W. S., & Dargan, P. I. (2011). Does cytochrome P450 liver isoenzyme induction increase the risk of liver toxicity after paracetamol overdose?. *Open access emergency medicine : OAEM*, 3, 69–76.
- Altschul SF, Wootton JC, Gertz EM, Agarwala R, Morgulis A, Schäffer AA, Yu YK. Protein database searches using compositionally adjusted substitution matrices. *FEBS J*. 2005 Oct;272(20):5101-9. doi: 10.1111/j.1742-4658.2005.04945.x. PMID: 16218944; PMCID: PMC1343503.
- Needleman SB & Wunsch CD (1970) A general method applicable to the search for similarities in the amino acid sequence of two proteins. *J Mol Biol* 48, 443–453.
- Altschul, S. F., Madden, T. L., Schäffer, A. A., Zhang, J., Zhang, Z., Miller, W., & Lipman, D. J. (1997). Gapped BLAST and PSI-BLAST: a new generation of protein database search programs. *Nucleic acids research*, 25(17), 3389–3402.
- Sievers, F., Wilm, A., Dineen, D., Gibson, T. J., Karplus, K., Li, W., Lopez, R., McWilliam, H., Remmert, M., Söding, J., Thompson, J. D., & Higgins, D. G. (2011). Fast, scalable generation of high-quality protein multiple sequence alignments using Clustal Omega. *Molecular systems biology*, 7, 539.
- Waterhouse A, Bertoni M, Bienert S, Studer G, Tauriello G, Gummienny R, Heer FT, de Beer TAP, Rempfer C, Bordoli L, Lepore R, Schwede T. SWISS-MODEL: homology modelling of protein structures and complexes. *Nucleic Acids Res*. 2018 Jul 2;46(W1):W296-W303. doi: 10.1093/nar/gky427.
- Bienert S, Waterhouse A, de Beer TA, Tauriello G, Studer G, Bordoli L, Schwede T. The SWISS-MODEL Repository-new features and functionality. *Nucleic Acids Res*. 2017 Jan 4;45(D1):D313-D319. doi: 10.1093/nar/gkw1132.
- Trott, O., & Olson, A. J. (2010). AutoDock Vina: improving the speed and accuracy of docking with a new scoring function, efficient optimization, and multithreading. *Journal of computational chemistry*, 31(2), 455–461.
- Aggunna and Yedidi (2022). *In silico* quantitative structure-activity relationship analysis of a highly potent experimental HIV-1 protease inhibitor, GRL10413. *TCABSE-J*, Vol. 1, Issue 3:10-17. Epub: Apr2nd, 2022.
- Yedidi, R. S., Maeda, K., Fyvie, W. S., Steffey, M., Davis, D. A., Palmer, I., Aoki, M., Kaufman, J. D., Stahl, S. J., Garimella, H., Das, D., Wingfield, P. T., Ghosh, A. K., & Mitsuya, H. (2013). P2' benzene carboxylic acid moiety is associated with decrease in cellular uptake: evaluation of novel nonpeptidic HIV-1 protease inhibitors containing P2 bis-tetrahydrofuran moiety. *Antimicrobial agents and chemotherapy*, 57(10), 4920–4927.
- Aggunna, M., Grandhi, A.V.K.S. and Yedidi, R.S. (2022). Artistic representation of Scientific data: prediction of mutant SARS-CoV-2 viral fitness based on the viral spike protein coding mRNA stability. *TCABSE-J*, Vol. 1, Issue 3:1-3. Epub: Apr 2nd, 2022
- Bond G. R. (2009). Acetaminophen protein adducts: a review. *Clinical toxicology (Philadelphia, Pa.)*, 47(1), 2–7.
- James, L. P., Letzig, L., Simpson, P. M., Capparelli, E., Roberts, D. W., Hinson, J. A., Davern, T. J., & Lee, W. M. (2009). Pharmacokinetics of acetaminophen-protein adducts in adults with acetaminophen overdose and acute liver failure. *Drug metabolism and disposition: the biological fate of chemicals*, 37(8), 1779–1784.